BUCK CONVERTER WITH VARIABLE INPUT VOLTAGE FOR PHOTOVOLTAIC APPLICATIONS

Marcelo Gradella Villalva , Ernesto Ruppert Filho
Universidade Estadual de Campinas (UNICAMP)
Campinas - SP- Brasil
mvillalv@dsce.fee.unicamp.br , ruppert@fee.unicamp.br

***Abstract* – This paper describes the modeling and control of a buck converter with variable input voltage. Some DC-DC converters for photovoltaic applications require that the input voltage be controlled while the output voltage is constant. This control is not so obvious and requires converter modeling and regulator design.**

***Keywords* – DC-DC, buck, control, photovoltaic, PV**

I. INTRODUCTION

Modeling and control of buck converters are two topics well known in the literature, which rise no challenges for researchers and engineers. However when the buck converter is used in photovoltaic applications the control system becomes complicated and requires modeling and controller design not readily available in the technical literature.

The purpose of this paper is to overcome the lack of information about modeling and controlling the input voltage of the buck converter when the output voltage remains constant.

The following sections will show the converter modeling with the state-space averaging method and will present the regulator design in details. The authors expect the readers will profit of this detailed analysis of the regulated-input buck converter and its control system.

Simulations are used to validate the buck converter linearized model and to test the performance of the designed closed-loop controller.

II. BUCK CONVERTER IN PV APPLICATIONS

Fig. 1 shows the simplified model of a photovoltaic (PV) array connected to a buck converter. The output voltage of the PV array is V_{PV}. This voltage must be controlled in order to keep the array operation at the maximum power point, which is accomplished by a power tracking algorithm (this subject is beyond the scope of this text). The maximum power point tracking (MPPT) algorithm provides the reference V_{PV}* for the buck converter. The buck converter sets the input voltage (which is the output voltage of the PV array) to the desired value while its output voltage is fixed.

In most typical applications of PV arrays the output of the array is directly connected to a load or to a battery with an approximately constant voltage. Although this kind of system is costless, the lack of the array output voltage control prohibits the system to operate at with maximum efficiency, hence energy is wasted. If a power electronic converter [1] is used to interface the PV array and the load (e.g. a battery that feeds a DC load or a DC-AC conversion stage) the best performance of the PV array may be achieved, hence the energy utilization is optimized.

This paper proposes a simple and also costless buck converter that may be used in PV applications where $V_{PV} > V_o$. For example, a PV cell whose voltage output varies between 20 *V* and 35 *V* may be interfaced to a 12 *V* battery by the buck converter.

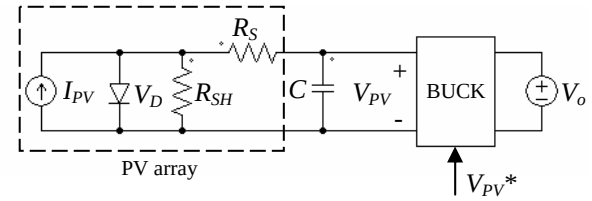

Fig. 1: PV array connected to a buck converter with constant output voltage.

Fig. 2 shows the buck converter. We can notice that, differently of conventional converters, the buck circuit of this figure has a constant output voltage and its input voltage depends on the output of the PV array. The voltage V_o may be kept constant by a battery or by another electronic power converter, as mentioned before.

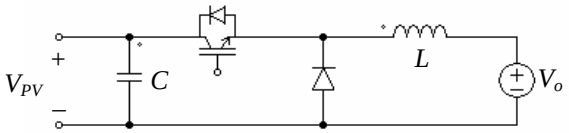

Fig. 2: Buck converter with variable input voltage.

III. SYSTEM MODELING

A. PV array

The simple PV array model [2,3] seen in Fig. 1 may have its diode removed in order to make easier the modeling process of the PV-buck system. In this case we consider that the PV array operates as a constant current source. However in a real situation the array will be forced to operate at the boundaries of the constant current and constant voltage modes if a maximum power tracker is employed. With this simplification the PV array may be represented by the simple Thévenin's equivalent circuit of Fig. 3. It is easier to use only one equivalent resistance R_{TH} instead of using the shunt (R_{SH}) and series (R_S) resistances of the original PV array model of Fig. 1. By using any of these models, with the current source I_{PV} or with the equivalent Thévenin's voltage V_{TH}, only one energy source will appear in the averaged model (current or

voltage source). These two models may be chosen arbitrarily and the following relations are valid.

$$R_{TH} = R_S + R_{SH} \quad (1)$$

$$V_{TH} = I_{PV} R_{SH} \quad (2)$$

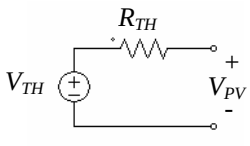

Fig. 3: Thévenin's equivalent circuit of the PV array operating as a constant current source.

B. Buck converter

1) State equations

The transistor of the buck converter of Fig. 2 switches according to the gate signal provided by the control system. When the switch is closed during the time interval $d.T$ the buck converter constitutes the circuit of Fig. 4a. When the transistor is open during the time interval $(1\text{-}d)T$ the circuit assumes the form of Fig. 4b. $f = 1/T$ is the switching frequency of the buck converter and d is the transistor duty cycle.

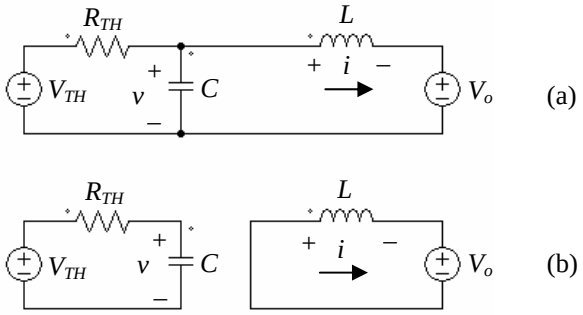

Fig. 4: (a) Buck converter when the transistor is conducting. (b) The same circuit when the transistor is open.

Each circuit of Fig. 4 may be described as a set of differential equations with two state variables: the capacitor voltage v and the inductor current i.

Equations (3) and (4) hold when the switch is closed.

Inductor: $$L\frac{di}{dt} = v - V_0 \quad (3)$$

Capacitor: $$C\frac{dv}{dt} = -\frac{v}{R_{TH}} + \frac{V_{TH}}{R_{TH}} - i \quad (4)$$

Equations (5) and (6) hold when the switch is open.

Inductor: $$L\frac{di}{dt} = -V_0 \quad (5)$$

Capacitor: $$C\frac{dv}{dt} = -\frac{v}{R_{TH}} + \frac{V_{TH}}{R_{TH}} \quad (6)$$

Equations (3) – (6) may be written in the state space form, as shown in equations (7) and (8).

$$\frac{d}{dt}\begin{bmatrix} i \\ v \end{bmatrix} = \underbrace{\begin{bmatrix} 0 & \frac{1}{L} \\ \frac{-1}{C} & \frac{-1}{C \cdot R_{TH}} \end{bmatrix}}_{\mathbf{A_1}} \cdot \begin{bmatrix} i \\ v \end{bmatrix} + \underbrace{\begin{bmatrix} 0 & 0 \\ 0 & \frac{-1}{C \cdot R_{TH}} \end{bmatrix}}_{\mathbf{B_1}} \cdot \begin{bmatrix} V_0 \\ V_{TH} \end{bmatrix} \quad (7)$$

$$\frac{d}{dt}\begin{bmatrix} i \\ v \end{bmatrix} = \underbrace{\begin{bmatrix} 0 & 0 \\ 0 & \frac{-1}{C \cdot R_{TH}} \end{bmatrix}}_{\mathbf{A_2}} \cdot \begin{bmatrix} i \\ v \end{bmatrix} + \underbrace{\begin{bmatrix} -\frac{1}{L} & 0 \\ 0 & \frac{1}{C \cdot RT_H} \end{bmatrix}}_{\mathbf{B_2}} \cdot \begin{bmatrix} V_0 \\ V_{TH} \end{bmatrix} \quad (8)$$

Matrices $\mathbf{A_1}$, $\mathbf{B_1}$ and $\mathbf{A_2}$, $\mathbf{B_2}$ are used to determine the $\mathbf{A}$ and $\mathbf{B}$ matrices of the averaged state equation. According to the state-space averaging method [4,5] we can write the averaged state equation (9), which is the weighted sum of equations (7) and (8). It is possible to write equations (10) and (11) because in every switching interval T of the buck transistor equation (7) is valid during $d.T$ and equation (8) is valid during $(1\text{-}d)T$. If the switching frequency of the transistor ($1/T$) is sufficiently high the averaged equations (9) – (11) may be used to describe the low frequency behavior of the circuit (with average currents and voltages). Vectors $\mathbf{x}$ and $\mathbf{u}$ in equation (9) contain average states and inputs of the circuit. Variables $<i>$ and $<v>$ are average states and V_0 and V_{TH} are DC values (we assume the input and output voltages have no AC components).

$$\dot{\mathbf{x}} = \mathbf{A} \cdot \mathbf{x} + \mathbf{B} \cdot \mathbf{u} \quad (9)$$

$$\mathbf{A} = \mathbf{A}_1 \cdot d + \mathbf{A}_2 \cdot (1-d) \quad (10)$$

$$\mathbf{B} = \mathbf{B}_1 \cdot d + \mathbf{B}_2 \cdot (1-d) \quad (11)$$

$$\mathbf{x} = \begin{bmatrix} < i > \\ < v > \end{bmatrix} \qquad \mathbf{u} = \begin{bmatrix} V_0 \\ V_{TH} \end{bmatrix} \quad (12)$$

2) DC values

Making $\dot{\mathbf{x}} = 0$, which is true when all transients have faded and the buck converter is in steady state, we obtain the DC equations (13) and (14) of the PV-buck system.

$$\mathbf{0} = \mathbf{A} \cdot \mathbf{X} + \mathbf{B} \cdot \mathbf{U} \quad (13)$$

$$\mathbf{X} = -\mathbf{A}^{-1} \cdot \mathbf{B} \cdot \mathbf{U} \quad (14)$$

From (14) we obtain (15), where I and V are the DC (steady state) values of <i> and <v>.

$$\mathbf{X} = \begin{bmatrix} I \\ V \end{bmatrix} = \begin{bmatrix} -V_0/(R_{TH}\cdot D^2) + V_{TH}/(R_{TH}\cdot D) \\ V_0/D \end{bmatrix} \quad (15)$$

The expression of V found in (15) is the well-known static input-to-output ratio of the buck converter.

3) Small signal analysis

In order to develop the control system of the buck converter it is necessary to obtain a converter model linearized at a chosen operating point. This linear model, which is valid for small signal variations, provides a linear transfer function that can be used in the design of the closed-loop control system.

The buck converter in this paper works in the voltage-control mode. The current-programmed mode could also have been considered, but it is not necessary unless we need to directly control the inductor current for any special purpose.

Generally the duty cycle d is used as the control variable in voltage-mode DC-DC converters. As we are concerned about the input voltage control, however, it is more convenient to obtain a model equation whose control variable is d', the complement of the transistor duty cycle given by equation (16), since positive variations of d produce negative variations of v.

$$d' = 1 - d \quad (16)$$

Let's make $d' = D' + \hat{d}'$, where D' is the DC value of d' and $\hat{d}'$ is a small signal AC perturbation. We wish to obtain a model that describes the behavior of the converter when small variations of the control variable occur, i.e. a linear model of the buck converter for the response to $\hat{d}'$ near the operating point D'. Let's also make $\mathbf{x} = \mathbf{X} + \hat{\mathbf{x}}$, where $\mathbf{x}$ is the averaged state vector, $\mathbf{X}$ contains the DC steady state values (I and V) and $\hat{\mathbf{x}}$ represents small state disturbances near the operating point $\mathbf{X}$. Similarly we can add small perturbations to the input $\mathbf{u}$ as shown in equation (19), but in this modeling we have assumed that $\hat{\mathbf{u}} = 0$.

$$d' = D' + \hat{d}' \quad (17)$$

$$\mathbf{x} = \mathbf{X} + \hat{\mathbf{x}} \quad (18)$$

$$\mathbf{u} = \mathbf{U} + \hat{\mathbf{u}} \quad (19)$$

The averaged equation of the PV-buck system may be written in function of the control variable d', as equation (20) shows.

$$\dot{\mathbf{x}} = \{\mathbf{A_1}\cdot(1\text{-}d') + \mathbf{A_2}\cdot d'\}\mathbf{x} + \{\mathbf{A_1}\cdot(1\text{-}d') + \mathbf{A_2}\cdot d'\}\cdot\mathbf{u} \quad (20)$$

Equation (21) is obtained by substituting (17) – (19) into (20), by ignoring the nonlinear terms and by applying the Laplace transform.

$$s\hat{\mathbf{x}}(s) = \mathbf{A}\hat{\mathbf{x}}(s) + \hat{d}'(s)\{(-\mathbf{A_1} + \mathbf{A_2})\mathbf{X} + (-\mathbf{B_1} + \mathbf{B_2})\mathbf{U}\} \quad (21)$$

From equation (21) we can obtain equation (22), which expresses the vector transfer function $\mathbf{G}(s)$.

$$\mathbf{G}(s) = \frac{\hat{\mathbf{x}}(s)}{\hat{d}'(s)} = \left(s\begin{bmatrix}1 & 0\\ 0 & 1\end{bmatrix} - \mathbf{A}\right)^{-1} \cdot \cdot \{(-\mathbf{A_1} + \mathbf{A_2})\mathbf{X} + (-\mathbf{B_1} + \mathbf{B_2})\mathbf{U}\} \quad (22)$$

From (22) the transfer functions $G_I(s) = \hat{i}(s)/\hat{d}'(s)$ and $G_V(s) = \hat{v}(s)/\hat{d}'(s)$ are obtained. G_V(s), the transfer function we are interested in, describes the response of the buck converter input voltage to small variations of d' around the operating point $V=V_0/D$, where D = 1- D'.

With some simple mathematical manipulations we can find the expression of the transfer function $G_V(s)$ seen in equation (23), where I and V are the DC steady state current and voltage from equation (15).

$$G_V(s) = \frac{R_{TH}(DV + sLI)}{s^2LCR_{TH} + sL + D^2R_{TH}} \quad (23)$$

IV. NUMERICAL EXAMPLE

A. Transfer function

Once we have found the transfer function $G_V(s)$, which gives the small signal response of the input voltage to the control variable d', let's analyze a numerical example.

The following parameter values – Tables 1 and 2 – will allow us to obtain a numerical transfer function through which the dynamic response of the converter may be studied.

Table 1

PV Cell	
R_{SH}	13.5620 Ω
R_S	0.2670 Ω
I_{PV}	19.2000 A
V_{TH}	260.3904 V
R_{TH}	13.8290 Ω

Table 2

Buck Converter	
L	0.0020 H
C	0.0015 F
V_0	15.0000 V
D	0.5000

Equation (24) shows the numerical transfer function of the buck converter with the PV array connected to its input.

$$G_V(s) = \frac{0.9216s + 207.4}{4.149e - 5s^2 + 0.002s + 3.457} \quad (24)$$

B. DC characteristic

Fig. 5 shows the static transfer characteristics of the real converter and of the linear model $G_V(s)$. This figure clearly shows that the transfer function is a linear model of the converter around the chosen operating point $D' = 0.5$.

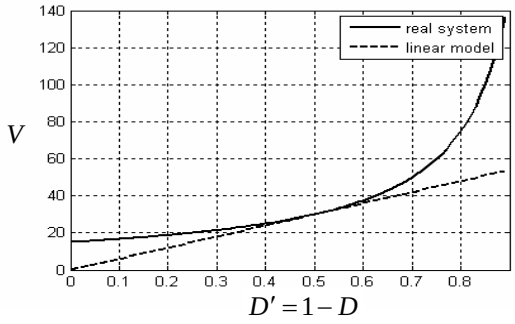

Fig. 5: Static characteristics of the real converter and of the linear model – transfer function $G_V(s)$.

Fig. 5 shows that the choice of $D' = 0.5$ is adequate because this is the midrange of the control variable and mainly because the derivatives of the static input voltage with respect to the control variable may become extremely low or extremely high as the operating point gets farther from $D' = 0.5$.

C. Open-loop dynamic response

Fig. 6 shows the open-loop step response of the real system and of the linear model $G_V(s)$. They are almost identical except at the higher peaks where the model error is bigger.

V. CLOSED-LOOP CONTROL SYSTEM

Fig. 7 shows the feedback closed-loop control system used to control the input voltage of the buck converter. As stated earlier the output of the PV array, whose voltage is V_{PV}, is connected to the input of the buck converter.

In the scheme of Fig. 7 $G_C(s)$ is the controller transfer function, $G_V(s)$ is the converter transfer function and $H(s)$ is the feedback transfer function. As we are focusing on the control theory and on the dynamic analysis of the converter, the gain of the pulse-width modulator (PWM) that controls the switch of the buck converter does not appear in the scheme of Fig. 7. As the plant input is the control variable d', the PWM is inherently modeled and its gain is unit.

The loop gain is $Gc(s)F(s)$, where $F(s) = G_V(s)H(s)$. For example let's make $H(s) = 0.02$, which corresponds to a voltage transducer with 1/50 conversion ratio and negligible dynamic characteristic.

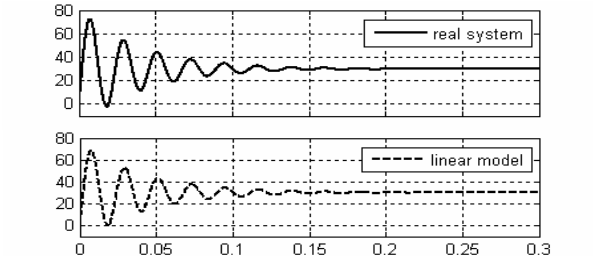

Fig. 6: Open-loop step response of the system composed of the PV array and the buck converter with constant output voltage.

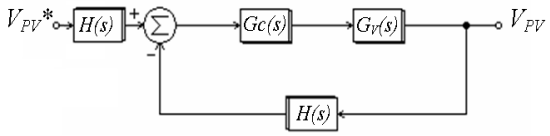

Fig. 7: Closed-loop control system for the buck converter.

A. PID regulator

This section shows the tuning process of the proportional integral derivative (PID) regulator used in the control system of the buck converter. The derivative compensator helps to improve the phase margin of the closed-loop system and consequently to improve the dynamic response and stability. The proportional compensator is used to increase the bandwidth of the system, which allows fast transient response. The integral compensator is necessary to warranty low steady-state error in the input voltage of the buck converter.

1) Proportional compensator

Fig. 8 shows the frequency response of $F(s)$. From this bode plot we can find the first-order approximation of the open-loop system by using the two asymptotes. This graphical method provides the open-loop cut-off frequency of the approximated first-order system, which is ω_0. The approximated first-order transfer function is $F_1(s)$ in equation (25), where G_{DC} is the DC gain of $F(s)$.

$$G_{V1}(s) = \frac{G_{DC}}{1 + s/\omega_0} \quad (25)$$

For high frequencies near and above ω_0 the transfer function of equation (25) may be approximated as $F_1(s)$ in equation (26).

$$F_1(s) \approx \frac{G_{DC}}{s/\omega_0} \quad (26)$$

The modulus of the approximated transfer function of equation (26) may be written as $\|F_1\|$ in equation (27).

$$\|F_1\| \approx \frac{G_{DC}}{\omega/\omega_0} \tag{27}$$

The purpose of the proportional compensator is to displace the bode plot vertically in order to set a new cross-over frequency for the closed-loop system, as Fig. 8 shows. By multiplying function *F(s)* by a factor K_P the bode plot is displaced upward and ω_C is the new cross-over frequency.

From equation (27) we can write an expression for K_P with the desired ω_C, equation (28).

$$K_P = \frac{\omega_C}{\omega_0 G_{DC}} \tag{28}$$

For the system studied in this paper, with the parameters given in Tables 1 and 2, we find $\omega_0 \approx 400\ rad/s$ and G_{DC} = 1.2. Let's design the closed-loop system for a cross-over frequency f_C = 1500 *Hz*, ω_C = 9.4248e+003 *rad/s*. This results K_P = 19.6350. Fig. 8 shows the bode plot of $F(s)K_P = G_V(s)H(s)K_P$. We can see that the cross-over frequency is ω_C = 8.7354e+003 *rad/s*, f_C = 1.3903e+003 *Hz*, very close to the desired frequency. This shows that the approximations made in equations (26) and (27) are reasonably good for practical purposes.

2) Integral compensator

The next step is to add a pole at the origin and a zero at an arbitrary low frequency so that the closed-loop system will have an infinite DC gain, thus allowing null steady state error for step inputs. The transfer function of the integral compensator is given by equation (29).

$$G_I = 1 + \frac{\omega_I}{s} = \frac{s + \omega_I}{s} \tag{29}$$

A good choice for the zero frequency is ω_I = 10 *rad/s*, which is much lower than ω_C. So the integral compensator will actuate at DC and low frequencies and will have practically no effect at high frequencies. Fig. 9 shows the bode plot of $F(s)K_P G_I(s)$.

3) Derivative compensator

Finally the derivative compensator can be used to improve the dynamic response by increasing the phase margin. The derivative transfer function $G_D(s)$ is given by equation (30).

$$G_D(s) = K_D \frac{(1 + s/\omega_Z)}{(1 + s/\omega_P)} \tag{30}$$

The transfer function $G_D(s)$ adds a pole and a zero to the system. The zero may be arbitrarily placed below the cross-over frequency ω_C. Let's say that $\omega_Z = \omega_C - \Delta\omega$, where $\Delta\omega$ must be chosen in order to achieve the desired phase margin reduction. After placing the zero we must choose the pole frequency so that the maximum phase displacement occurs exactly at ω_C. From the control systems theory [6,7] we know that $\omega_C = \sqrt{\omega_Z \cdot \omega_P}$, so we can write equation (31).

$$\omega_P = \omega_C{}^2 / \omega_Z \tag{31}$$

The derivative gain K_D must be chosen so that $G_D(s)$ does not cause any gain increase to the compensated system, as the cross-over frequency has already been determined by the proportional gain K_P. The gain K_D is given by equation (32).

$$K_D = \sqrt{\omega_Z / \omega_P} \tag{32}$$

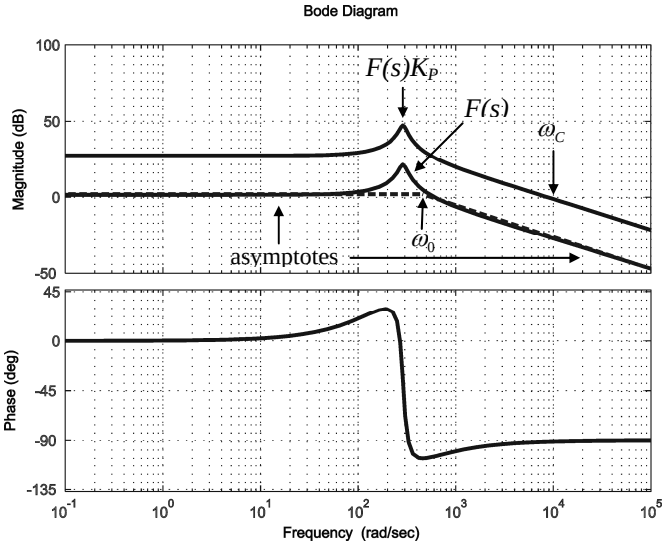

Fig. 8: Frequency responses of *F(s)* and $F(s)K_P$.

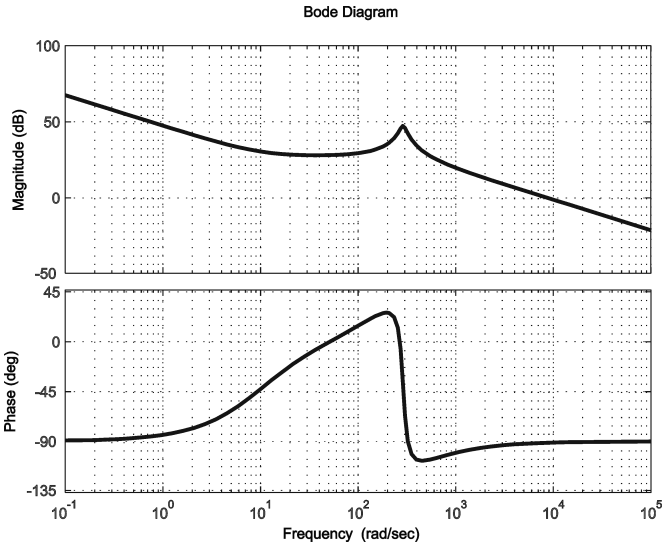

Fig. 9: Frequency response of $F(s)K_P G_I(s)$.

For the system studied in this paper, with the parameters of Tables 1 and 2, with $\Delta\omega$ = 3000 *rad/s*, we have: ω_Z = 5.7354e+003 rad/s, ω_P = 1.3305e+004 rad/s, K_D = 0.6566. Fig. 10 shows the Bode plot of the system loop gain with the addition of the derivative compensator, where we can notice that the phase margin is improved without any changes to the magnitude of the frequency response, i.e. the previously determined cross-over frequency remains fixed even with the addition of the derivative compensator $G_D(s)$.

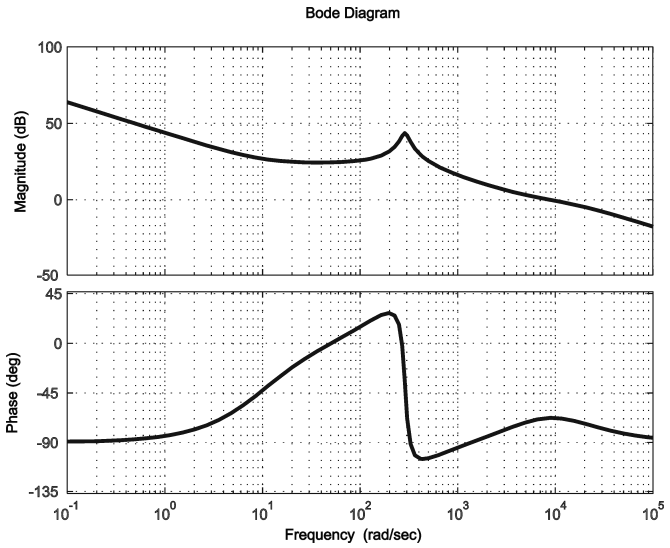

Fig. 10: Frequency response of $F(s)K_PG_I(s)G_D(s)$.

4) Regulator transfer function

The desired PID regulator transfer function is finally given by equation (33).

$$G_C(s) = K_P \cdot G_I(s) \cdot G_D(s) \qquad (33)$$

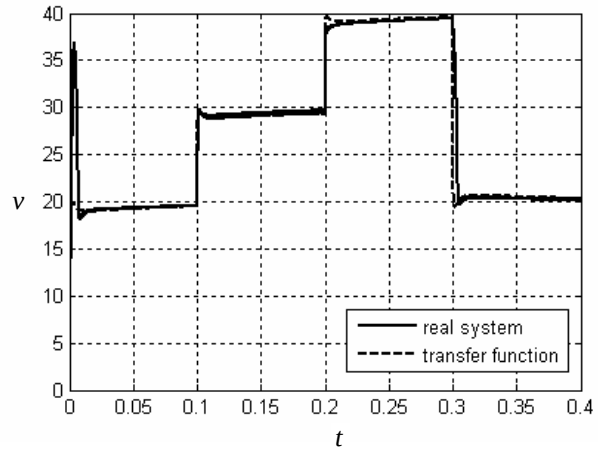

Fig. 11: Responses of the closed-loop system to input steps at t = 0 *s*, t = 0.1 *s*, t = 0.2 *s* and t = 0.3 *s*.

VI. RESULTS

With the regulator designed in the previous section the buck converter connected to the PV array attains fast transient response, negligible steady state error and excellent stability (assured by the large phase margin of the compensated system). Fig. 11 shows the step responses of a simulated converter and of the closed-loop transfer function of equation (34).

$$G_{CL}(s) = G_V(s) / \{1 + G_V(s)H(s)G_C(s)\} \qquad (34)$$

VII. CONCLUSIONS

This paper has shown how a buck converter with input voltage control is modeled with the state space averaging method. Very few papers in the literature deal with the input control of DC-DC converters. The detailed modeling process presented here is rarely found elsewhere. Another contribution, although minor, is the modeling with the control variable d' instead of d. This paper has also presented very comprehensive instructions for the design of the PID regulator used in the closed-loop control system of the buck converter.

The step responses presented in Fig. 6 show that the linear model exactly describes the behavior of the real system near the operating point. The step responses of Fig. 11 show that the closed-loop system of Fig. 7 works perfectly with the designed PID compensator.

REFERENCES

[1] C. Prapanavarat, M. Barnes, N. Jenkins, “Investigation of the Performance of a Photovoltaic AC Module”, *IEE Proc.-Gener. Transm. Ditrib.*, vol. 149, no. 4, July 2002.

[2] F. Nakanishi, T. Ikegami, K. Ebihara, S. Kuriyama, Y. Shiota, “Modeling and Operation of a 10 kW Photovoltaic Power Generator Using Equivalent Electric Circuit Method”, Proc. IEEE Photovoltaic Specialists Conference, 2000.

[3] C. Hua, J. R. Lin, “DSP-Based Controller Application in Battery Storage of Photovoltaic System”, Proc. IEEE IECON, 1996.

[4] R. D. Middlebrook, S. Cuk, “A General Unified Approach to Modeling Switching-Converter Power Stages”, International Journal of Electronics, vol. 42, no. 6, pp. 521-550, June 1977.

[5] R. W. Erickson, D. Maksimovic, “Fundamentals of Power Electronics”, Kluwer Academic Publishers, 2nd Edition, ISBN 0-7923-7270-0.

[6] C. L. Philips, R. D. Harbor, “Feedback Control Systems”, Prentice Hall, 3rd Edition, 1996, ISBN 0-13-371691-0.

[7] G. Franklin, J. D. Powell, A. Emami-Naeini “Feedback Control of Dynamic Systems”, 3rd Edition, Addison Wesley, 1995, ISBN 0-201-52747-2.